

Original Paper

# Genome analysis and gene expression profiling of neuroblastoma and ganglioneuroblastoma reveal differences between neuroblastic and Schwannian stromal cells

Simona Coco,<sup>1</sup> Raffaella Defferrari,<sup>2</sup> Paola Scaruffi,<sup>1,2</sup> Andrea Cavazzana,<sup>3</sup> Claudio Di Cristofano,<sup>3</sup> Luca Longo,<sup>1</sup> Katia Mazzocco,<sup>2</sup> Patrizia Perri,<sup>2</sup> Claudio Gambini,<sup>4</sup> Stefano Moretti,<sup>5</sup> Stefano Bonassi<sup>5</sup> and Gian Paolo Tonini<sup>1\*</sup>

<sup>1</sup>Unit of Translational Paediatric Oncology, National Institute for Cancer Research (IST), Largo R Benzi 10, 16132 Genoa, Italy

<sup>2</sup>Laboratory of Italian Neuroblastoma Foundation, Advanced Biotechnology Center (ABC), Largo R Benzi 10, 16132 Genoa, Italy

<sup>3</sup>Section of Molecular Pathology, Division of Oncology, Pisa University Hospital, Via Roma 57, 56126 Pisa, Italy

<sup>4</sup>Department of Pathology, Gaslini Children's Hospital, Largo G Gaslini 5, 16147 Genoa, Italy

<sup>5</sup>Unit of Molecular Epidemiology, National Institute for Cancer Research (IST), Largo R Benzi 10, 16132 Genoa, Italy

\*Correspondence to:

Gian Paolo Tonini, Unit of Translational Paediatric Oncology, National Institute for Cancer Research (IST), Largo R Benzi, 10, 16132 Genoa, Italy.  
E-mail: gianpaolo.tonini@istge.it

## Abstract

Neuroblastic tumours are a group of paediatric cancers with marked morphological heterogeneity. Neuroblastoma (Schwannian stroma-poor) (NB-SP) is composed of undifferentiated neuroblasts. Ganglioneuroblastoma intermixed (Schwannian stroma-rich) (GNBi-SR) is predominantly composed of Schwannian stromal (SS) and neuroblastic (Nb) cells. There are contrasting reports suggesting that SS cells are non-neoplastic. In the present study, laser capture microdissection (LCM) was employed to isolate SS and Nb cells. Chromosome 1p36 deletion and *MYCN* gene amplification were found to be associated in two out of seven NB-SPs, whereas no abnormalities were observed in five GNBi-SRs. In some cases, loss of heterozygosity (LOH) at 1p36 loci was detected in Nb cells but not in the bulk tumour by LCM; furthermore, LOH was also identified in both SS and tumour tissue of a GNBi-SR. DNA gain and loss studied by comparative genomic hybridization were observed at several chromosome regions in NB-SP but in few regions of GNBi-SR. Finally, gene expression profiles studied using an oligo-microarray technique displayed two distinct signatures: in the first, 32 genes were expressed in NB-SP and in the second, 14 genes were expressed in GNBi-SR. The results show that NB-SP is composed of different morphologically indistinguishable malignant cell clones harbouring cryptic mutations that are detectable only after LCM. The degree of DNA imbalance is higher in NB-SP than in GNBi-SR. However, when the analysis of chromosome 1p36 is performed at the level of microdissection, LOH is also observed in SS cells. These data provide supportive evidence that SS cells have a less aggressive phenotype and play a role in tumour maturation.

Copyright © 2005 Pathological Society of Great Britain and Ireland. Published by John Wiley & Sons, Ltd.

**Keywords:** neuroblastoma; loss of heterozygosity; comparative genomic hybridisation; gene expression profiling; laser capture microdissection; Schwann cell; neuroblastic cell

Received: 19 April 2005  
Revised: 8 June 2005  
Accepted: 23 June 2005

## Introduction

Neuroblastic tumours (NTs) are a group of paediatric cancers with great morphological heterogeneity. Shimada *et al* [1,2] classified NTs into four categories: neuroblastoma, ganglioneuroblastoma intermixed, ganglioneuroblastoma nodular, and ganglioneuroblastoma, according to the degree of cell maturation. The most common NTs are neuroblastoma (Schwannian stroma-poor) (NB-SP), where the stroma is poorly represented. Among the remaining categories, the most common histological type is ganglioneuroblastoma intermixed (Schwannian stroma-rich) (GNBi-SR), a tumour composed predominantly of Schwannian stromal cells within which nests of neuroblastic (Nb) cells are embedded [2].

Children over 1 year of age with NB-SP have a poor prognosis, whereas younger children with NB-SP or GNBi-SR generally have a better prognosis [3]. Furthermore, the morphological differences between these two tumours correlate with different biological patterns. *MYCN* amplification has been found frequently in NB-SP, whereas it is rarely observed in GNBi-SR [4–7]. Marked heterogeneity of *MYCN* gene amplification has also been reported in different areas of the same tumour [8,9] and in tumours from the same patient with multifocal neuroblastoma [10].

Chromosome 1p deletion has been observed at a frequency ranging between 20% and 80%, and associated with *MYCN* amplification [11–13]. Moreover, additional numerical and structural chromosome

abnormalities have also been detected in NB-SP [14–16].

Ganglioneuroblastomas (GNBs) rarely show chromosome abnormalities. Goto *et al* [4] analysed 21 GNBs and none of them had *MYCN* amplification. We have observed 47 GNBs and found only one tumour with focal *MYCN* amplification and one with 1p36 deletion (data not shown). Ambros *et al* [17] have suggested that Schwannian stromal (SS) cells of GNB are not neoplastic cells but rather a reactive cell recruited from the tumour environment. According to Ambros *et al*, the Schwannian cell should be able to release soluble factors, inducing the maturation of malignant neuroblasts. Recently, Liu *et al* [18] have demonstrated that murine Schwann cells are able to promote human neuroblast differentiation. The presence of a large number of SS cells in tumours with favourable histology and their absence in those with unfavourable histology [2] further support this hypothesis [17].

This issue has been challenged by Mora *et al* [19], who showed that SS cells, as well as Nb cells, may harbour DNA abnormalities, suggesting that both cells are malignant and that they are derived from a common pluripotent progenitor cell.

The histological and biological heterogeneity of NTs is associated with a variable clinical outcome and with a different response to chemotherapy [20]. For this reason, improved understanding of genotype–phenotype relationships in NTs will help to better define patients at risk of relapse and to improve patient management.

In the last decade, the advent of laser capture microdissection (LCM) has allowed the microdissection of tumour tissue areas using a focused laser beam [21,22]. The absence of any mechanical contact prevents cell-by-cell contamination and microdissected cells can be used directly for nucleic acid purification. This technique has been successfully applied in several cancers [21,22], including neuroblastoma [23].

We have studied *MYCN* gene and chromosome 1p36 status in NB-SP and GNBi-SR and have employed LCM to isolate Nb and SS cells. DNA purified from Nb and SS cells was used to study loss of heterozygosity (LOH) for chromosome 1p36 using microsatellite markers and for genome-wide analysis by comparative genomic hybridization (CGH).

Furthermore, we used oligo-microarray technology to identify differences in gene expression between NB-SP and GNBi-SR. This powerful technique has been employed in studies of several malignancies [24,25] and neuroblastoma [26–29]. Ohira *et al* [27] identified 305 genes differentially expressed between favourable and unfavourable NTs.

Our results show that the degree of genetic abnormality is higher in NB-SP than in GNBi-SR; moreover, LOH for chromosome 1p36 was observed in laser microdissected cells from both Nb and SS. Finally, gene expression analysis using microarrays showed a different signature between NB-SP and GNBi-SR.

## Materials and methods

### Tumour samples and laser tissue microdissection

Twelve primary tumours, seven NB-SPs and five GNBi-SRs, were obtained from patients at different clinical stages [30]. The study protocol was approved by local and international ethics committees. Informed consent to use surgical specimens for research purposes was obtained from each patient. Tumours were classified according to the International Neuroblastoma Pathology Committee (INPC) [1]. We used frozen and paraffin-embedded samples with a cell content ranging between 60% and 90% in NB-SP and between 3% and 10% in GNBi-SR.

LCM was performed on paraffin-embedded tissues specimens. Tissue sections of 6 µm were stained with Mayer's haematoxylin. The AS-LMD Laser System (Leica Microsystems, Wetzlar, Germany) was used to isolate tumour areas containing Nb or SS cells. From 200 to 500 cells were captured for each sample.

### DNA and RNA purification

DNA from tumour and peripheral blood lymphocytes of the corresponding patient were purified with phenol and chloroform as previously described [7]. RNA for microarray analysis was extracted by using the Perfect RNA Eukaryotic Kit (Eppendorf, Hamburg, Germany). Microdissected cells were collected in a tube and DNA was extracted using the QIAamp® DNA Micro kit (Qiagen GmbH, Hilden, Germany).

### Determination of DNA index

DNA content was analysed by a cytofluorimeter (FAC-Scan Becton Dickinson) and at least 20 000 events were recorded. We used 40 µm thick representative paraffin sections from each tumour. After digestion of the section in pepsin solution at 1%, the cell suspension was stained with propidium iodide (50 mg/l), Triton X-100 (1 ml/l), and RNase (75 kU/ml). The results were analysed using Modfit software [31].

### Double colour fluorescence *in situ* hybridization (FISH) in interphase nuclei

Imprints of fresh tumours were used for the analysis of chromosome 1p36 deletion (chromosome 1p36 minisatellite probe, Direct Labelled and Chromosome 1 Satellite Probe, Direct Red; Qbiogene, Illkirch Cedex, France) and *MYCN* amplification (chromosome 2p24 (*MYCN*)/Alpha Satellite 2 Cocktail Probe, Dual Colour, Direct Labelled; Qbiogene). FISH scoring for chromosome 1p36 and *MYCN* was according to Ambros *et al* [32].

### Study of allelic loss at chromosome 1p36 using D1S80 and D1S76 markers

LOH was studied with a PCR-based method using primers for D1S80 and D1S76 loci, which map to the

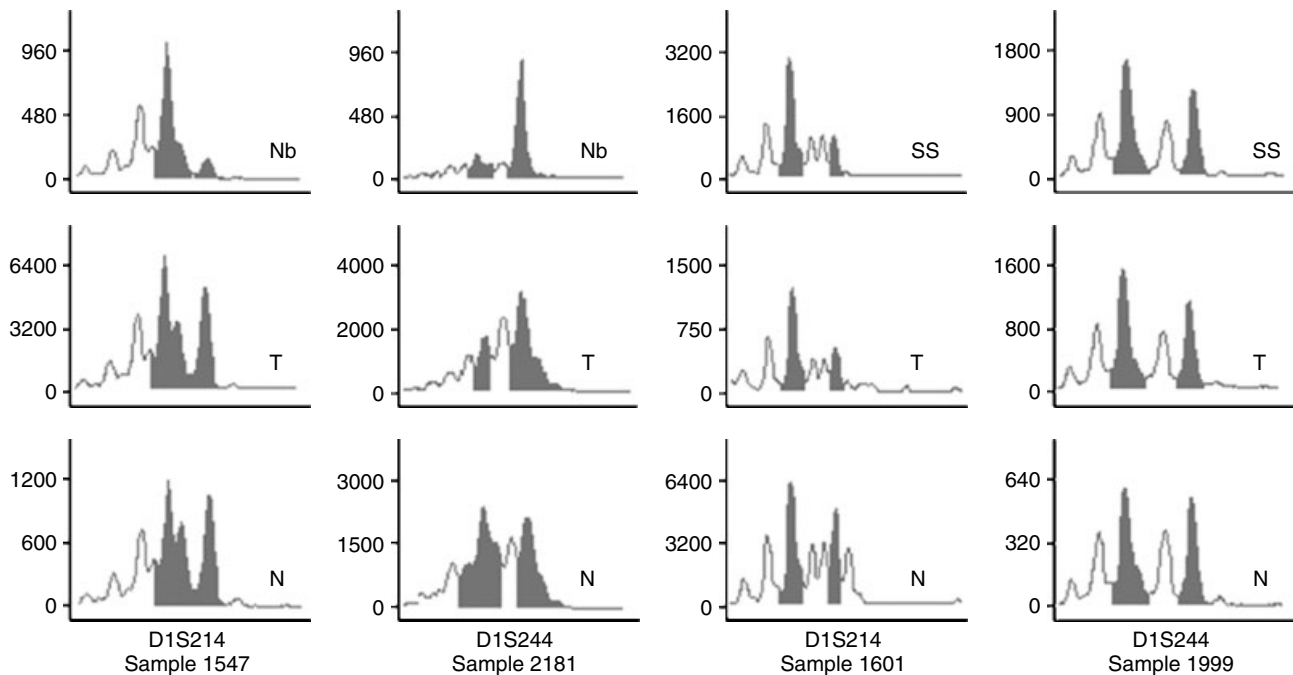


**Figure 1.** Analysis of microsatellites (D1S214 and D1S244) in neuroblastoma (Schwannian stroma-poor) and ganglioneuroblastoma (Schwannian stroma-rich). For sample 1547, LOH was detected in the microdissected neuroblastic cells (Nb) but not in the whole tumour (T); for samples 2181 and 1601, LOH was found in both Nb and Schwannian stromal (SS) cells and in the whole tumour; for sample 1999, heterozygosity was retained for both cell types. N = normal DNA. Patient tumour and blood electropherograms were compared to determine LOH according to the following formula: (area normal allele 1/area normal allele 2)/(area tumour allele 1/area tumour allele 2). LOH was defined as a score of  $\leq 0.5$  or  $\geq 2$

sub-telomeric region of chromosome 1p36, according to Peter *et al* [33].

#### Genome analysis by comparative genomic hybridization

CGH was performed as described by Kallioniemi *et al* [34]. Briefly, tumour and control DNA were labelled by nick translation with biotin-16-dUTP (Roche Diagnostic GmbH, Mannheim, Germany) and digoxigenin-11-dUTP (Roche Diagnostic GmbH), respectively. Equal amounts of labelled control and tumour DNA, together with 30  $\mu$ g of Cot-1 DNA (Roche Diagnostic GmbH) and 1  $\mu$ g of salmon sperm DNA, were precipitated with ethanol. Labelled DNA probes were dissolved in hybridization buffer, denatured at 80°C for 5 min, and then applied to denatured metaphase slides obtained from healthy individuals. After a 3-day incubation, slides were washed and hybridization signals were revealed with avidin-fluorescein isothiocyanate and mouse anti-digoxigenin antibodies. Metaphases were counterstained with 4',6-diamidino-2-phenolindole in Vectashield Mounting Medium (Vector Lab, Burlingame, CA, USA). Digital images were collected using a computer-controlled E800 fluorescence microscope (Nikon Instruments, Firenze, Italy) using the Genikon System (Nikon Instruments).

#### Degenerate oligonucleotide primed (DOP)-PCR

DNA isolated from microdissected cells was amplified using DOP-PCR. The reaction was carried out in two

steps as previously described by Kuukasjarvi *et al* [35] with minor modifications. In the first step, the 10 $\times$  high salt buffer was replaced with Thermo Sequenase reaction buffer (Amersham, Buckinghamshire, UK). In the second step, the 10 $\times$  low salt buffer and Ampli-Taq polymerase were replaced with 10 $\times$  PCR buffer and Platinum Taq DNA Polymerase (Invitrogen Corp, CA, USA), respectively. The total cycle number of amplification was increased from 30 to 35.

#### Analysis of the chromosome 1p36 region using CA repeat markers

Tumour DNA, patient normal matched DNA, and DOP-PCR product were screened for the following markers: D1S468, D1S214, D1S244, and D1S228, mapping to the 1p36.3–36.2 region. Only sample 1554 was studied further using the additional markers: D1S507, D1S436, and D1S199, mapping to the 1p36.2–p36.1 region. PCR was performed with 0.8  $\mu$ M of each fluorescent primer, 0.2 mM of each dNTP, 2 mM MgCl<sub>2</sub>, 1 $\times$  GeneAmp Buffer II, 0.12 units of Ampli-Taq Gold (Perkin-Elmer Applied BioSystem, Foster City, CA, USA), and 1–3  $\mu$ l of DOP amplified or 60 ng of genomic DNA. Amplification was carried out under the following conditions: initial denaturation at 95°C for 12 min; ten cycles of 94°C  $\times$  25 s, 55°C  $\times$  25 s, 72°C  $\times$  30 s; 25 cycles of 90°C  $\times$  25 s, 55°C  $\times$  20 s, 72°C  $\times$  30 s; and a final extension at 72°C for 20 min. The product was analysed using a Multicapillary Sequencer ABI 3100 (Applied BioSystem, Foster City, CA, USA). Data were analysed with

Genescan and Genotyper software package (Applied BioSystem).

Microarray experiments for gene expression analysis

We applied the ‘small sample target labelling protocol’ to amplify and to label targets from total RNA samples for GeneChip® probe array expression analysis (www.affymetrix.com) [36]. The protocol utilizes two cycles of standard cDNA synthesis combined with *in vitro* transcription for target amplification. The first cycle provides initial amplification of total RNA, resulting in unlabelled cRNA. In the second cycle of synthesis, biotin ribonucleotides are incorporated to produce labelled antisense cRNA target.

Double-stranded cDNA from total RNA was synthesized using the SuperScript cDNA Synthesis kit (Invitrogen Corp). A high-quality HPLC-purified T7-(dT)<sub>24</sub> oligomer (MWG-Biotech AG, Ebersberg, Germany) was used for priming first-strand cDNA synthesis. We produced the biotin-labelled antisense copy RNA (cRNA) using the BioArray™ HighYield™ RNA Transcript Labeling Kit (Enzo Diagnostics, Inc, NY, USA). The *in vitro* transcription reaction was performed using T7 RNA polymerase and biotin-labelled nucleotides. After cleaning up using the RNeasy Mini Kit (Qiagen, MD, USA) and quantification, the biotinylated cRNA was aliquoted in a reaction buffer containing Tris-acetate (pH 8.1), KOAc, and MgOAc. An aliquot of double-stranded cDNA, of cRNA and of biotinylated cRNA was analysed for size distribution and yield on an agarose gel. In order to identify unscheduled hybridizations, each sample was tested with a test chip containing eukaryotic control sequences including housekeeping genes. Then each sample was probed with the Human Genome U133A GeneChip® (Affymetrix, Inc, CA, USA). After pre-hybridization, both single test and standard probe arrays were hybridized with the biotinylated cRNA hybridization cocktail at 45 °C for 16 h in the Affymetrix GeneChip® Hybridization Oven 640. Probe array washing and staining were performed in the Fluidics station. Each chip was stained with a streptavidin–phycoerythrin conjugate and read with the GeneChip® laser confocal fluorescence scanner. Image acquisition and image analysis were performed using the Affymetrix® Microarray Suite Software.

Statistical analysis

Human Genome 133A GeneChip® intensity data were transformed for normalization and variance stabilization by the VSN (variance stabilization normalization) [37] method implemented in Bioconductor software (http://www.bioconductor.org). We also performed cluster analysis using the R package and the NetAffy Gene Ontology Mining Tool.

Table 1. DNA cell content, MYCN gene status, and analysis of chromosome 1p36 region of neuroblastoma (Schwannian stroma-poor)

Code	DNA index	MYCN status	Signal ratio FISH 1p36	Neuroblastoma (Schwannian stroma-poor)													
				Minisatellites 1p36							Microsatellites 1p36						
				DIS80	DIS76	DIS468	DIS468	DIS214	DIS214	DIS244	DIS244	DIS244	DIS228	DIS228	DIS228	DIS228	
1528	1.43	NA	3/3 73% 2/2 12% 3/2 12% 4/4 3%	No LOH	No LOH	No LOH	LOH	ni	ni	ni	No LOH	No LOH	No LOH	No LOH	No LOH	No LOH	
1538	1.00	A	2/1 96% 2/2 4%	LOH	ni	ni	ni	ni	ni	ni	LOH	LOH	LOH	LOH	LOH	No LOH	
1547	1.46	NA	3/3 49% 2/2 4% 4/4 3% 3/2 6% 4/2 2.5% 4/3 35.5%	No LOH	No LOH	No LOH	LOH	ni	No LOH	LOH	No LOH	No LOH	No LOH	No LOH	No LOH	No LOH	No LOH
1548	nd	NA	3/3 59% 2/2 29% 4/4 8% 3/2 1% 2/3 3%	No LOH	No LOH	No LOH	No LOH	ni	ni	ni	LOH	LOH	LOH	LOH	LOH	No LOH	
1554	1.07	NA	2/2 86.5% 3/3 4.5% 4/4 5% 2/1 2% 3/2 1% 1/2 1%	No LOH	No LOH	ni	ni	ni	ni	ni	No LOH	No LOH	No LOH	No LOH	No LOH	No LOH	No LOH
2181	nd	A	3/2 75% 2/2 21% 3/3 2% 4/3 2%	LOH	LOH	LOH	LOH	LOH	LOH	LOH	ni	ni	ni	LOH	LOH	LOH	
2215	nd	NA	2/2 78.5% 2/1 11.5% 3/3 2% 3/2 2% 2/3 2.5% 1/1 + 1/2 3.5%	ni	No LOH	No LOH	LOH	No LOH	No LOH	LOH	No LOH	No LOH	LOH	LOH	ni	ni	ni
<b>Total</b>		<b>Amplified Deleted</b>															<b>LOH</b>
7		2/7	2/7	1/5	2/7	1/5	4/5	1/3	3/3	2/6	5/6	1/6	1/6	1/6	1/6	1/6	

Code = Tumour sample code; MYCN status: NA = not amplified; A = amplified. Signal ratio FISH: ratio between signals of chromosome 1 centromeric probe and DIS22 subtelomeric probe. No LOH = no loss of heterozygosity; LOH = loss of heterozygosity; ni = not informative; T = whole tumour; Nb = neuroblastic microdissected cells; nd = not detected.

**Table 2.** DNA cell content, MYCN gene status, and analysis of chromosome 1p36 region of ganglioneuroblastoma intermixed (Schwannian stroma-rich)

Ganglioneuroblastoma, Intermixed (Schwannian stroma-rich)																			
Microsatellites 1p36																			
Code	DNA index	MYCN status	Signal Ratio FISH 1p36	Minisatellites 1p36			DIS468			DIS214			DIS244			DIS228			
				DIS80 T	DIS76 T	T	Nb	SS	T	Nb									
1601	1.00	NA	2/2 7.4% 3/3 18% 4/4 4% 1/2 4%	ni	No LOH	No LOH	No LOH	No LOH	LOH	No LOH	No LOH	LOH	No LOH	LOH	No LOH	No LOH	ni	ni	ni
1915	1.00	NA	2/2 82% 3/2 12% 2/1 3% 2/3 3%	No LOH	No LOH	No LOH	nd	No LOH	No LOH	No LOH	No LOH	nd	No LOH	No LOH	nd	No LOH	ni	ni	ni
1999	1.27	NA	2/2 69% 3/3 11% 2/1 3% 3/2 17%	nd	No LOH	No LOH	nd	No LOH	ni	No LOH	ni	nd	No LOH	ni	nd	No LOH	No LOH	nd	No LOH
2004	1.17	NA	2/2 81% 3/2 7% 3/3 4% 2/1 3% 1/2 3% 4/4 2%	No LOH	No LOH	ni	ni	ni	ni	No LOH	No LOH	nd	No LOH	No LOH	nd	No LOH	ni	ni	ni
2258	nd	NA	2/2 71% 3/3 8% 4/4 8% 2/1 2% 3/2 3% 4/2 4% 2/4 + 2/3 4%	No LOH	ni	ni	ni	ni	ni	No LOH									
<b>Total</b>			<b>Amplified Deleted</b>																
5		0/5	0/5	0/3	0/3	0/3	0/1	0/3	1/4	0/1	0/1	1/4	0/5	0/1	0/5	0/1	0/2	0/1	0/2

Code = Tumour sample code; MYCN status: NA = not amplified; A = amplified. Signal ratio FISH: ratio between signals of chromosome 1 centromeric probe and DIZ2 subtelomeric probe. No LOH = no loss of heterozygosity; LOH = loss of heterozygosity; ni = not informative. T = whole tumour; Nb = neuroblastic microdissected cells; SS = Schwann stromal microdissected cells; nd = not detected.

## Results

### MYCN amplification and chromosome 1p36 status in NB-SP and GNBi-SR tumours

The results of genomic analysis of seven NB-SPs and five GNBi-SRs are reported in Tables 1 and 2, respectively. The DNA content observed in NB-SP (Table 1) ranged between 1.00 and 1.46. Both *MYCN* amplification and 1p36 deletion were detected by FISH in tumour samples 1538 and 2181. Deletion of 1p36 was also observed in 11% of the tumour cells of sample number 2215. FISH 1p36 imbalance was detected in samples 1528 and 1547. Allelic loss was observed at the D1S76 locus of tumour 1538 and at the D1S76 and D1S80 loci of sample 2181. No LOH was detected at the same loci of samples 1528, 1547, 1548, and 1554.

Trisomy of chromosome 1 as determined by fluorescent centromeric/telomeric signal ratio was frequently observed in all cases, with a frequency ranging from 2% to 73% of tumour nuclei. A similar result was found for chromosome 2 (data not shown).

Three of four samples (1601, 1915, and 2004) from GNBi-SR tumours were diploid or nearly diploid (Table 2). No *MYCN* amplification was observed in any of the five GNBi-SRs. All GNBi-SRs had a disomic chromosome 1 content in most cells (signal ratio 2/2 in more than 70% of nuclei). Chromosome 1p36 FISH imbalance was detected in two cases (1915 and 1999). No LOH at D1S80 and D1S76 loci was observed in any of the GNBi-SRs.

### Chromosome 1p36 status in NB-SP tumours

In order to define the 1p36 status better in whole tumours and Nb cells of NB-SP, we used CA repeat markers covering a region of 13.40 Mb (<http://www.ncbi.nlm.nih.gov/genome>) from telomere to 1p36.21 (Table 1, Figure 1). All specimens were informative for at least two markers. 1p36 LOH was detected in three of seven cases in both T and Nb tissue cells, whereas in three cases (1547, 1528, and 2215), allelic loss at 1p36 was detectable only in Nb cells. In particular, we were able to identify allelic loss at

the D1S468 and D1S244 loci in the microdissected Nb cells of case 1528, which had a chromosome 1p36 imbalance restricted to 12% of tumour cells, and in tumour 2215, which showed 1p36 FISH abnormalities restricted to 11% of nuclei.

### Chromosome 1p36 status in SS of GNBi-SR

For GNBi-SR tumours, we identified allelic loss at the D1S214 locus in both microdissected SS and in whole tumour specimens in only one case (sample 1601). No LOH was detected in the remaining GNBi-SRs (Table 2, Figure 1).

### Genome-wide analysis of NB-SP and GNBi-SR

The results of CGH analyses performed in T and Nb specimens of NB-SPs are reported in Table 3. Loss of the 1p32-pter and 1p3s-p36.2 regions were detected in T and Nb, respectively, of sample 1554 (Figure 2). Furthermore, several numerical and structural aberrations were observed in both whole tumours and Nb cells of the other NB-SPs. Heterogeneous genetic abnormalities were observed in whole tumour and neuroblastic cells. Sample 1538 shows 2p24 gain in the whole tumour and in Nb cells, but Nb cells also have gains at 5q13-23, 17, 18p, and 19 chromosome regions. On the other hand, loss at 2q22-31, 5q15, and 11q14-qter was found in tumour 2215 but the microdissected Nb cells showed no losses, whereas 7q33-pter, 17, and 18 gains were detected in the whole tumour and 17, 18 gain in Nb (Table 3).

Few chromosome abnormalities were observed in GNBi-SRs by CGH analysis (Table 4). Sample 1915 showed loss at 1p35 and monosomy of chromosome 16, while loss of chromosome 16p was found in sample 2258. The remaining tumours did not show any DNA gains or losses.

### Gene expression profile of NB-SP and GNBi-SR

We used Affymetrix Human Genome U133A chips to select genes differentially expressed between NB-SP and GNBi-SR. Cluster analysis was performed employing a hierarchical clustering algorithm. After data normalization, the expression values of the

**Table 3.** Comparative genomic hybridization analysis of neuroblastoma (Schwannian stroma-poor)

Code	Chromosome region			
	Loss		Gain	
	T	Nb	T	Nb
1528	Normal	nd	17	nd
1538	Normal	Normal	2p24	2p24; 5q13-23; 17; 18p; 19
1547	16;19	Normal	12q15-21	19
1548	16	nd	Normal	nd
1554	1p32-pter; 17p11-12; 19	1p33-p36.2	11q21-qter	4q21-27; 18p
2181	Normal	nd	2p23-pter	nd
2215	2q22-31; 5q15; 11q14-qter	Normal	7q33-qter; 17; 18	17; 18

Code = tumour sample code; T = whole tumour; Nb = neuroblastic microdissected cells; nd = not detected.



**Figure 2.** Example of a CGH ideogram performed on bulk tumour (A) and LCM tumour cells (B) from sample 1554 (see also Table 3). Red and green arrows indicate the chromosome regions with DNA loss and DNA gain, respectively. Three-colour images representing tumour DNA (green), reference DNA (red), and DAPI counter-stain (blue) were captured. Sixteen to 30 metaphases were analysed as separate grey-scale images. Green and red fluorescence intensities were then scored along the vertical medial axis of each chromosome. For evaluation of CGH data, the average ratio (SD limit of 95%) and the individual ratio profiles were analysed. Chromosomes X and Y were excluded from the analysis. CGH controls were performed by matching two normal donors' DNA

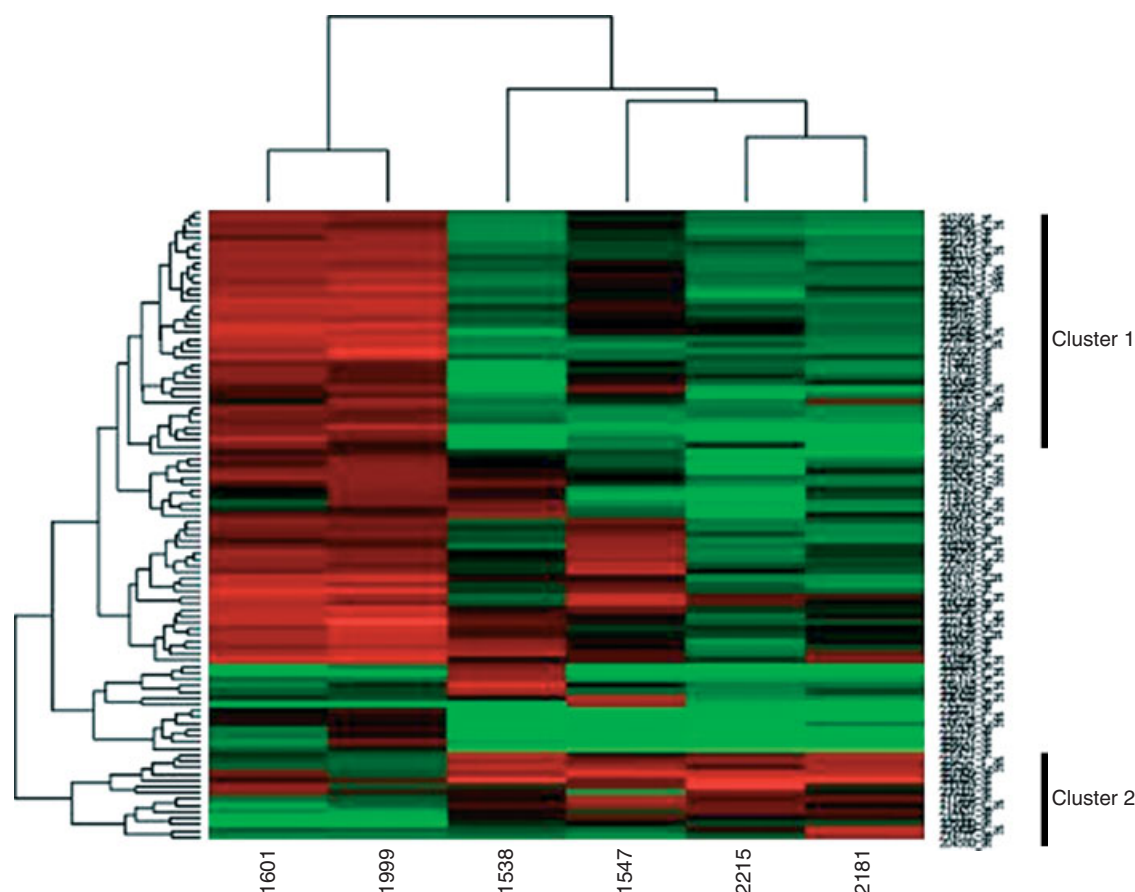


**Figure 3.** Hierarchical clustering dendrogram of expression data. Each colour patch in the resulting visual map represents the expression level of the associated gene in that tumour sample, with a continuum of expression levels from dark green (lowest) to bright red (highest). The colour map indicates that this hierarchy is associated with distinct groupings of increased gene expression intensity (clusters 1 and 2). Cluster 1: a cluster of genes that are more intensely expressed in GNB-SR than in NB-SP tumours. Cluster 2: a cluster of genes that are more highly expressed in SP-NB samples than in GNB-SPs

**Table 4.** Comparative genomic hybridization analysis of ganglioneuroblastoma (Schwannian stroma-rich)

Chromosome region		
Code	Loss	Gain
1601	Normal	Normal
1915	1p35; 16	Normal
1999	Normal	Normal
2004	Normal	Normal
2258	16p	Normal

Code = tumour sample code; T = whole tumour; Nb = neuroblastic microdissected cells; nd = not detected.

50 probes with the highest standard deviation are shown in the false colour image (Figure 3) on a red–black–green scale (red: high expression value; black: middle expression value; green: low expression value). Rows and columns have been ordered according to the computation of an agglomerative clustering based on the ‘furthest neighbour’ method.

The NB-SPs and GNB-SRs are placed on different trunks and these tumours are also separated from one another, occupying adjacent branches of the same trunk. Thus, the hierarchical cluster algorithm, operating on a relatively small set of expression data,

was completely successful in grouping the two types of NTs on the basis of subtle distributed differences in gene expression. Figure 3 indicates that two clusters, 1 and 2, appear to drive the separation between the NB-SP and GNB-SR samples. Table 5 lists the genes of cluster 1 and Table 6 those of cluster 2.

Gene ontology is widely accepted as the standard vocabulary for describing the biological process, molecular function, and cellular component for genes. We used the Affymetrix Gene Ontology Mining Tool to map GeneChip probe sets to these hierarchical vocabularies to annotate genes and to provide a graphical view of probe-set representation within the biological process of genes [38].

Cluster 1 comprises 32 genes that were more intensely expressed in GNB-SRs than in NB-SPs. These genes code for proteins involved in cell adhesion (*CDH19*, *CDH1*, *NRXN3*), cell–cell signalling (*ADCYAP1*, *CALCA*, *SST*, *VIP*), immune response (*MBP*), neuropeptide hormone activity (*CRH*), signal transduction (*MAL*, *RGS1*, *TM4SF3*), and differentiation (*SI00B*).

Cluster 2 contains 14 genes that were more highly expressed in NB-SPs than in GNB-SRs. This cluster contains genes coding for transcription factors, including the mycn oncoprotein, rpl18a and rps4y1

**Table 5.** Transcripts expressed in GNB-SR tumours. List of 32 transcripts of cluster 1 found to be more expressed in GNB-SR than in NB-SP tumours, selected by hierarchical analysis

Symbol	Accession number	Description	Biological function
ASPA	M21692	Aspartoacyclase	Aminoacyclase activity
PTPRZ1	NM_002851	Protein tyrosine phosphatase, receptor-type, Z polypeptide 1	Carbonate dehydratase activity
CDH19	NM_003607	Cadherin 19, type 2	Cell adhesion
CDH1	BC065910	Cadherin 1, type 1	cell adhesion
NRXN3	NM_004796	Neurexin 3	Cell adhesion
ADCYAP1	NM_004010	Dystrophin	Cell-cell signalling
CALCA	BF447272	Calcitonin	Cell-cell signalling
SST	NM_001048	Somatostatin	Cell-cell signalling
VIP	NM_003381	Vasoactive intestinal peptide	Cell-cell signalling
IL8	NM_000584	Interleukin 8	Chemokine Activity
PCSK1	NM_000439	Proprotein convertase subtilisin/kexin type 1	Hydrolase activity
MBP	M13577	Myelin basic protein	Immune response
S100B	BC001766	S100 calcium binding protein, neural	Cell cycle progression and differentiation
LGII	NM_005097	Leucine-rich, glioma inactivated 1	Neurogenesis
CRH	NM_006614	Corticotropin-releasing hormone	Neuropeptide hormone activity
ERBB3	M29366	v-erb-b2 avian erythroblastic leukaemia viral oncogene homologue 3	Protein amino acid phosphorylation
TTID	NM_006790	Titin immunoglobulin domain protein	Protein binding
MAFF	NM_012323	v-maf musculoaponeurotic fibrosarcoma oncogene family, protein F	Regulation of transcription
CDT6	NM_004360	Angiotensin-like factor	Response to oxidative stress
MAL	NM_002371	mal, T-cell differentiation protein	Signal transduction
RGS1	NM_002922	Regulator of G-protein signalling 1	Signal transduction
TM4SF3	NM_004616	Transmembrane 4 superfamily member 3	Signal transduction
DMD	BC012049	Dystrophin	Structural constituent of cytoskeleton
KRT19	NM_002276	Keratin 19	Structural molecule activity
BTEB1	NM_000049	Basic transcription element binding protein 1	Transcription factor activity
EGR3	NM_015310	Early growth response 3	Transcription factor activity
NR4A2	NM_006186	Nuclear receptor subfamily 4, group A, member 2	Transcription factor activity
PMP2	NM_002677	Peripheral myelin protein 2	Transporter activity
GPRI05	NM_014879	Purinergic receptor P2Y, G-protein coupled, 14	UDP-activated nucleotide receptor activity
C8ORF4	NM_020130	Chromosome 8 open reading frame 4	—
PHLDA1	BC018929	Pleckstrin homology-like domain, family A, member 1	—
PLP1	BC002665	Proteolipid protein 1	—

**Table 6.** Transcripts expressed in NB-SP tumours. List of 14 transcripts of cluster 2 found to be more expressed in NB-SP than in GNB-SR tumours, selected by hierarchical analysis

Symbol	Accession number	Description	Biological function
NPY	NM_000905	Neuropeptide Y	Cell proliferation
TMSNB	NM_021992	Thymosin, beta, identified in neuroblastoma cells	Cytoskeleton organization and biogenesis
HIST1H2BG	BC001131	Histone 1, H2bg	DNA binding
DDX3Y	NM_004660	DEAD (Asp-Glu-Ala-Asp) box polypeptide 3, Y-linked	Nucleic acid binding
MMP12	NM_002426	Matrix metalloproteinase 12 (macrophage elastase)	Proteolysis and peptidolysis
EYA1	AJ000098	Eyes absent homologue 1 ( <i>Drosophila</i> )	Regulation of transcription
RPL18A	NM_000980	Ribosomal protein L18a	RNA binding
RPS4Y1	NM_001008	Ribosomal protein S4, Y-linked 1	RNA binding
EIF1AY	BC005248	Eukaryotic translation initiation factor 1A, Y-linked	RNA binding
MYCN	BC002712	v-myc myelocytomatosis viral-related oncogene, neuroblastoma-derived (avian)	Transcription factor activity
TFAP2B	NM_003221	Transcription factor AP-2 beta (activating enhancer binding protein 2 beta)	Transcription factor activity
ISL1	NM_002202	ISL1 transcription factor, LIM/homeodomain (islet-1)	Transcription factor activity
my048	AF063606	my048 protein	—
IGKC	AA777793	Immunoglobulin kappa light chain VKJ region	—

ribosomal proteins, and neuropeptide Y protein related to cell proliferation.

## Discussion

NTs are characterized by morphological and genetic heterogeneity. In order to understand better the

relationship between genotype and phenotype of NTs, we have studied seven cases of NB-SP and five of the GNB-SR subtype, using laser capture microdissection, CGH, and oligo-microarray technology.

Four of seven NB-SPs showed chromosome 1 trisomy and since tumours were composed of more than 90% of neuroblastic cells, this trisomy is most likely

associated with the neuroblastic cells. On the other hand, all five GNBi-SRs showed a 2/2 chromosome 1p36 FISH ratio in the overwhelming majority of nuclei. These tumours were composed of more than 90% of SS cells and chromosome 1p disomy has been associated with Schwannian stromal cells. Our data appear to endorse the DNA content cellular profile of NTs proposed by Ambros *et al* [17], with Schwann cells having a 2n DNA content while the Nb cells are characterized by 3n DNA. We used the LCM technique to break down the apparently uniform tumour tissue of NB-SPs and to show that it is composed of different malignant cellular clones that are morphologically indistinguishable but exhibit different genetic abnormalities. The presence of different neuroblastic clones is also supported by the heterogeneous distribution of *MYCN* gene amplification (data not shown) and chromosome 1p36 deletion (data presented) observed within the same tumour. Ambros *et al* [8] reported a heterogeneous distribution of *MYCN* gene amplification in several neuroblastomas, showing that they are composed of different cell subpopulations; Mora *et al* [20] demonstrated clonal heterogeneity of tumour cells at the onset of disease and at patients' relapse after therapy. Results presented here and our experience from the study of chromosome 1p36 and *MYCN* status in more than 150 neuroblastomas (data not shown) indicate a high degree of intratumoural genetic heterogeneity.

In particular, it is noteworthy that the LCM technique allowed us to detect allelic deletions in Nb cells that were not detected in bulk tumour. The presence of these cryptic mutations may partially explain the aggressive behaviour of those NTs that show neither *MYCN* amplification nor chromosome 1p36 deletion by FISH analysis.

CGH analysis showed loss of the 1p32-pter and 1p33-p36.2 regions in whole tumours and Nb cells, respectively, of sample 1554. The deletion was confirmed by LOH analysis at loci D1S507, D1S436, and D1S199, which map to a more centromeric 1p36.13 region (data not shown).

CGH also provided unexpected information in GNBi-SR samples. In fact, we detected loss at chromosome 1p35 (case 1915) and chromosome 16 (cases 1915 and 2258) in this tumour subtype. Using the same technique, Toraman *et al* [39] observed gains at 2p25-pter, a region corresponding to the *MYCN* locus, in five cases of ganglioneuroblastoma. Furthermore, LOH at the D1S214 locus was found in microdissected SS cells of GNBi-SR (case 1601). Our observation may explain the presence of LOH in localized tumour with favourable histology, as reported by Iolascon *et al* [12] and Martinsson *et al* [13]. Taken together, these findings argue against the hypothesis that SS cells in GNBs are reactive and non-neoplastic [17].

In conclusion, we have shown that NB-SPs and GNBi-SRs are characterized by distinct patterns of genetic abnormality. NB-SPs have a higher degree of

genetic instability than previously suspected. This is present at different levels, including cryptic 1p36 deletions detectable only in neuroblastic cells isolated by microdissection. Therefore, a given NB-SP tumour can be thought of as an expansion of multiple clones that have diverse differentiation capabilities and therapeutic responsiveness.

The degree of genetic instability is much lower in favourable NTs such as GNBi-SR. This low level of instability may justify the apparent normality of SS and the less aggressive nature of the tumour. Oligo-microarray is a potent tool for identifying sets of genes differently expressed in two cell phenotypes simultaneously. We have employed this microarray technology to evaluate the signatures of NB-SP and GNBi-SR tumours. A hierarchical cluster algorithm generated two types of NT on the basis of differences in gene expression and the two most obvious clusters appeared to drive the separation between NB-SP and GNBi-SR samples.

Interestingly, S100 calcium binding protein beta (S100B, OMIM 176990) is expressed more highly in GNBi-SR tumours than in NB-SP tumours. S100B belongs to the large family of S100 proteins [40,41] and its expression has been detected in SS cells and associated with favourable histological types [42-44]. This protein is also associated with neuroblastoma cell maturation, being induced in human neuroblastoma cell lines stimulated with 5-bromo-2'-deoxyuridine [42,43]. This suggests that Schwann cells present in neuroblastoma and expressing S100 protein are stroma-derived cells. S100B protein could therefore be one of the differentiating factors proposed by Ambros *et al* [17] in the model of neuroblastoma maturation. Another gene that is significantly highly expressed in GNBi-SR is somatostatin (OMIM 182450). Recently, Pola *et al* [45] have demonstrated that somatostatin plays an anti-migratory and anti-invasive role in neuroblastoma cells, suggesting that it plays a role in the favourable development of GNBi-SR. Our findings, together with the results reported by Liu *et al* [18], strongly support the role of Schwannian cells as a promoter of neuroblastoma cell differentiation.

Genes expressed more highly in NB-SP tumours code for several transcription factors, ribosomal proteins, and proteins related to cell proliferation. One of these transcription factors is the *mycn* oncoprotein. This finding supports the role of *MYCN* gene expression in the neuronal phenotype rather than in more mature neural-derived cells [46]. Interestingly, we found high expression of neuropeptide Y in NB-SP samples. An increased plasma level of npy protein was observed in patients with neuroblastoma at relapse of disease [47] and it has been suggested that this protein plays a role in the dissemination of neuroblastoma cells [48]. Finally, our results give new information about the genotype-phenotype relationships of neuroblastic and Schwann stromal cells.

## Acknowledgements

This work was supported by Fondazione Italiana per la Lotta al Neuroblastoma, Associazione Italiana per la Ricerca sul Cancro (AIRC), Ministero dell'Università e della Ricerca Scientifica e Tecnologica (MURST), Ministero della Sanità (DIA4-CIPE).

## References

- Shimada H, Ambros IM, Dehner LP, Hata J, Joshi VV, Roald B. Terminology and morphologic criteria of neuroblastic tumors: recommendations by the International Neuroblastoma Pathology Committee. *Cancer* 1999;**86**:349–363.
- Shimada H, Umehara S, Monobe Y, Hachitanda Y, Nakagawa A, Goto S, et al. International neuroblastoma pathology classification for prognostic evaluation of patients with peripheral neuroblastic tumors: a report from the Children's Cancer Group. *Cancer* 2001;**92**:2451–2461.
- Peuchmaur M, d'Amore ES, Joshi VV, Hata J, Roald B, Dehner LP, et al. Revision of the International Neuroblastoma Pathology Classification: confirmation of favorable and unfavorable prognostic subsets in ganglioneuroblastoma, nodular. *Cancer* 2003;**98**:2274–2281.
- Goto S, Umehara S, Gerbing RB, Stram DO, Brodeur GM, Seeger RG, et al. Histopathology (International Neuroblastoma Pathology Classification) and MYCN status in patients with peripheral neuroblastic tumors: a report from the Children's Cancer Group. *Cancer* 2001;**92**:2699–2708.
- Seeger RC, Brodeur GM, Sather H, Dalton A, Siegel SE, Wong KY, et al. Association of multiple copies of the N-myc oncogene with rapid progression of neuroblastomas. *N Engl J Med* 1985;**313**:1111–1116.
- Brodeur GM, Hayes FA, Green AA, Casper JT, Wasson J, Wallach S, et al. Consistent N-myc copy number in simultaneous or consecutive neuroblastoma samples from sixty individual patients. *Cancer Res* 1987;**47**:4248–4253.
- Tonini GP, Boni L, Pession A, Rogers D, Iolascon A, Basso G, et al. MYCN oncogene amplification in neuroblastoma is associated with worse prognosis, except in stage 4s. The Italian experience with 295 children. *J Clin Oncol* 1997;**15**:85–93.
- Ambros PF, Ambros IM, Kerbl R, Luegmayr A, Rumpler S, Ladenstein R, et al. Intratumoral heterogeneity of 1p deletions and MYCN amplification in neuroblastomas. *Med Pediatr Oncol* 2001;**36**:1–4.
- Brodeur GM. Significance of intratumoral genetic heterogeneity in neuroblastomas. *Med Pediatr Oncol* 2002;**38**:112–113.
- Casciano I, Ponzoni M, Lo Cunsolo C, Tonini GP, Romani M. Different p73 splicing variants are expressed in distinct tumor areas of a multifocal neuroblastoma. *Cell Death Differentiation* 1999;**6**:391–393.
- Caron H, Van Sluis P, De Kraker J, Bokkerink J, Egeler M, Laureys G, et al. Allelic loss of chromosome 1p as a predictor of unfavorable outcome in patients with neuroblastoma. *N Engl J Med* 1996;**334**:225–230.
- Iolascon A, Lo Cunsolo C, Giordani L, Cusano R, Boumgartner M, Ghisellini P, et al. Interstitial and large chromosome 1p deletion occurs in neuroblastoma of patients with both localized and disseminated tumours and predicts an unfavourable outcome. *Cancer Lett* 1998;**130**:83–92.
- Martinsson T, Sjöberg RM, Hedborg F, Kogner P. Deletion of chromosome 1p loci and microsatellite instability in neuroblastomas analyzed with short-tandem repeat polymorphisms. *Cancer Res* 1995;**55**:5681–5686.
- Brodeur GM. Neuroblastoma: biological insights into a clinical enigma. *Nature Rev Cancer* 2003;**3**:203–216.
- Tonini GP, Romani M. Genetic and epigenetic alterations in neuroblastoma. *Cancer Lett* 2003;**197**:69–73.
- Schwab M, Westermann F, Hero B, Berthold F. Neuroblastoma: biology and molecular and chromosomal pathology. *Lancet Oncol* 2003;**4**:472–480.
- Ambros IM, Zellner A, Roald B, Amann G, Ladenstein R, Printz D, et al. Role of ploidy, chromosome 1p, and Schwann cells in the maturation of neuroblastoma. *N Engl J Med* 1996;**334**:1505–1511.
- Liu S, Tian Y, Chlenski A, Yang Q, Zage P, Salwen HR, et al. Cross-talk between Schwann cells and neuroblasts influences the biology of neuroblastoma xenografts. *Am J Pathol* 2005;**166**:891–900.
- Mora J, Cheung NK, Juan G, Illei P, Cheung I, Akram M, et al. Neuroblastic and Schwannian stromal cells of neuroblastoma are derived from a tumoral progenitor cell. *Cancer Res* 2001;**61**:6892–6898.
- Mora J, Cheung NK, Gerald WL. Genetic heterogeneity and clonal evolution in neuroblastoma. *Br J Cancer* 2001;**85**:182–189.
- Fend F, Raffeld M. Laser capture microdissection in pathology. *J Clin Pathol* 2000;**53**:666–672.
- Curran S, McKay JA, McLeod HL, Murray GI. Laser capture microscopy. *Mol Pathol* 2000;**53**:64–68.
- De Preter K, Vandesompele J, Heimann P, Kockx MM, Van Gele M, Hoebek J, et al. Application of laser capture microdissection in genetic analysis of neuroblastoma and neuroblastoma precursor cells. *Cancer Lett* 2003;**197**:53–61.
- Raetz EA, Moos PJ. Impact of microarray technology in clinical oncology. *Cancer Invest* 2004;**22**:312–320.
- Luo J, Isaacs WB, Trent JM, Duggan DJ. Looking beyond morphology: cancer gene expression profiling using DNA microarrays. *Cancer Invest* 2003;**21**:937–949.
- Khan J, Wei JS, Ringner M, Saal LH, Ladanyi M, Westermann F, et al. Classification and diagnostic prediction of cancers using gene expression profiling and artificial neural networks. *Nature Med* 2001;**7**:673–679.
- Ohira M, Morohashi A, Inuzuka H, Shishikura T, Kawamoto T, Kageyama H, et al. Expression profiling and characterization of 4200 genes cloned from primary neuroblastomas: identification of 305 genes differentially expressed between favorable and unfavourable subsets. *Oncogene* 2003;**22**:5525–5536.
- Hiyama E, Hiyama K, Yamaoka H, Sueda T, Reynolds CP, Yokoyama T. Expression profiling of favorable and unfavorable neuroblastomas. *Pediatr Surg Int* 2004;**20**:33–38.
- Takita J, Ishii M, Tsutsumi S, Tanaka Y, Kato K, Toyoda Y, et al. Gene expression profiling and identification of novel prognostic marker genes in neuroblastoma. *Genes Chromosomes Cancer* 2004;**40**:120–132.
- Brodeur GM, Pritchard J, Berthold F, Carlsen NL, Castel V, Castelberry RP, et al. Revision of the international criteria for neuroblastoma diagnosis, staging and response to treatment. *J Clin Oncol* 1993;**11**:1466–1477.
- Marshall T, Rutledge JC. Flow cytometry DNA applications in pediatric tumor pathology. *Pediatr Dev Pathol* 2000;**3**:314–334.
- Ambros IM, Benard J, Boavida M, Bown N, Caron H, Combaret V, et al. Quality assessment of genetic markers used for therapy stratification. *J Clin Oncol* 2003;**21**:2077–2084.
- Peter M, Michon J, Vielh P, Neuenschwander S, Nakamura Y, Sonsino E, et al. PCR assay for chromosome 1p deletion in small neuroblastoma samples. *Int J Cancer* 1992;**52**:544–548.
- Kallioniemi OP, Kallioniemi A, Sudar D, Rutovitz D, Gray JW, Waldman F, et al. Comparative genomic hybridization: a rapid new method for detecting and mapping DNA amplification in tumors. *Semin Cancer Biol* 1993;**4**:41–46.
- Kuukasjarvi T, Tanner M, Pennanen S, Karhu R, Visakorpi T, Isola J. Optimizing DOP-PCR for universal amplification of small DNA samples in comparative genomic hybridization. *Genes Chromosomes Cancer* 1997;**18**:94–101.
- Eberwine J, Yeah H, Miyashiro K, Cao Y, Nair S, Finnel R, et al. Analysis of gene expression in single live neurons. *Proc Natl Acad Sci U S A* 1992;**89**:3010–3014.
- Ross I, Gentleman R. A language for data analysis and graphics. *J Comput Graph Stat* 1996;**5**:299–314.
- Ashburner M, Ball CA, Blake JA, Botstein D, Butler H, Cherry JM, et al. Gene ontology: tool for the unification of biology. The Gene Ontology Consortium. *Nature Genet* 2000;**25**:25–29.

39. Toraman AD, Toraman AD, Keser I, Luleci G, Tunalı N, Gelen T. Comparative genomic hybridization in ganglioneuroblastomas. *Cancer Genet Cytogenet* 2002;**132**:36–40.
40. Heizmann CW, Fritz G, Schafer BW. S100 proteins: structure, functions and pathology. *Front Biosci* 2002;**7**:1356–1368.
41. Marshak DR. S100 beta as a neurotrophic factor. *Prog Brain Res* 1990;**86**:169–181.
42. Misugi K, Aoki I, Kikyo S, Sasaki Y, Tsunoda A, Nakajima T. Immunohistochemical study of neuroblastoma and related tumors with anti-S-100 protein antibody. *Pediatr Pathol* 1985;**3**:217–226.
43. Katsetos CD, Karkavelas G, Frankfurter A, Vlachos IN, Vogelely K, Schober R, *et al.* The stromal Schwann cell during maturation of peripheral neuroblastomas. Immunohistochemical observations with antibodies to the neuronal class III beta-tubulin isotype (beta III) and S-100 protein. *Clin Neuropathol* 1994;**13**:171–180.
44. Tsunamoto K, Todo S, Imashuku S, Kato K. Induction of S 100 protein by 5-bromo-2'-deoxyuridine in human neuroblastoma cell lines. *Cancer Res* 1988;**48**:170–174.
45. Pola S, Cattaneo MG, Vicentini LM. Anti-migratory and anti-invasive effect of somatostatin in human neuroblastoma cells: involvement of Rac and MAP kinase activity. *J Biol Chem* 2003;**278**:40 601–40 606.
46. Edsjo A, Nilsson H, Vandesompele J, Karlsson J, Pattyn F, Culp LA, *et al.* Neuroblastoma cells with overexpressed MYCN retain their capacity to undergo neuronal differentiation. *Lab Invest* 2004;**84**:406–417.
47. Dotsch J, Christiansen H, Hanze J, Lampert F, Rascher W. Plasma neuropeptide Y of children with neuroblastoma in relation to stage, age and prognosis, and tissue neuropeptide Y. *Regul Pept* 1998;**75**:185–190.
48. Kogner P, Borgstrom P, Bjellerup P, Schilling FH, Refai E, Jonsson C. Somatostatin in neuroblastoma and ganglioneuroma. *Eur J Cancer* 1997;**33**:2084–2089.